Analysis of Emitted Electromagnetic Interference of DC Electric Vehicle Supply Equipment

Tycho van Leersum
ElaadNL
University of Twente
Arnhem, The Netherlands
tychovanleersum@gmail.com

***Abstract*—High-power electric vehicle chargers are being installed on a large scale. These devices use converters that convert AC power to DC power. They generate distortion in the supraharmonic spectrum which can cause varying issues. This research measured and characterized the emission of three high-power electric vehicle chargers under different operating conditions using various analysis methods. The chargers are also tested against proposed emission limits. The results varied significantly between EVSEs. Results show a distortion's amplitude and frequency can change over time. These findings can be used when developing feasible standards for the regulatory gap.**

***Index Terms*—EMI, power quality, supraharmonic distortion, supraharmonic current, DC EVSE, operating conditions, time-frequency analysis**

I. Introduction

Transitioning from fossil fuels to renewable energy sources poses many challenges. One of these challenges is the electrification of the transport sector, which is achieved by replacing internal combustion engine vehicles with electric vehicles (EVs). A common reason for consumers against purchasing EVs is the limited range. This issue can be solved by installing DC electric vehicle supply equipment (EVSE) along highways. These devices can reach higher charging speeds than conventional chargers, allowing drivers to increase their range significantly in a 15-minute break. The difference between conventional and fast charging is that conventional charging uses the onboard charger (OBC) in the EV to convert the AC grid power to DC, while fast charging uses a DC EVSE to perform the conversion. The OBC is located in the car, which limits its weight and size. DC EVSEs do not have this restriction, allowing them to charge at over 300 kW. A fast-charging plaza with tens of these devices can easily draw several megawatts at peak consumption. This threatens the electricity grid's power quality as converters are notorious for generating distortion in the supraharmonic (SH) range [1].

Power quality rules regulate electromagnetic interference (EMI) below 2 kHz, while electromagnetic compatibility (EMC) regulations apply to frequencies above 150 kHz. This leaves a regulatory gap between 2 kHz and 150 kHz, known as the SH frequency range [2]. Although the name "supraharmonic" suggests it concerns distortion at integer multiples of the grid frequency, the SH frequency range is a continuous spectrum. Though the spectrum is not regulated yet, supraharmonic distortion (SHD) can cause problems such as unwanted tripping of earth leakage current breakers, failure of measurement instruments, audible noise, and undesired switching of lighting [3] [4]. Because of these effects, proper standards must be devised to limit SHD.

Currently, EMC compliance testing is often conducted using an EMI receiver. This device is connected to the device under test (DUT) and measures its distortion. The distortion is analyzed in the frequency domain by applying an analog bandpass filter and measuring the total emission in the band. The size of these bands is called the resolution bandwidth (RBW). The RBW changes depending on the frequency. For example, it could be 200 Hz below 9 kHz and 5 MHz between 30 and 300 MHz. The EMI receiver sweeps through the spectrum and measures one band at a time. A few quantities are determined during a measurement, such as peak and average distortion. Measuring all bands creates a graph of these quantities over frequency. These graphs are compared to limits to determine if the DUT is compliant. Each band is measured consecutively, so one sweep through the spectrum is time-consuming. Since the DUT may have hundreds of different settings and operating conditions that all have to be tested, the compliance test can take a long time. The specific procedure and all variables such as the RBW and the limits of the EMI are defined in standards like the IEC61000-4-7[5]. These standardizations allow for a fair comparison between DUTs, but that does not imply that the test environments described in the standards represent realistic scenarios. The standards for the SH range must be designed to provide fair and repeatable results. This can be achieved by analyzing the behavior of SHD to determine which behaviors the tests need to account for. The limits must be set at an achievable level for manufacturers, but also such that few EMC issues arise.

In [6], current emission limits, also known as the "Slangen limits", are proposed for the SH range on an installation level. This means they apply to the total emission of, for example, a charging plaza. The limits are derived from research on realistic grid impedances and the IEC 61000-2-2, which states voltage

compatibility limits. The limits can vary based on the grid impedance at the connection point of the installation. To not exceed the installation limit when connecting multiple devices, individual devices are recommended to remain below 25% of the installation limit.

Several ways to analyze SHD exist, such as supraharmonic current (SHC), total supraharmonic current (TSHC), supraharmonic voltage (SHV), and total supraharmonic voltage (TSHV). In [7], the SHCs of an EVSE for several operating conditions are measured. They found a strong correlation between emitted SHC and the DC output voltage of the EVSE. The output power did not affect the emitted SHC.

In [8], the SHD of various OBCs in frequency and time domain are characterized. They analyzed the voltage distortion from 9 kHz to 500 kHz. They found the amplitude of the distortion was time-dependent and repeated itself over time.

This research aims to provide insight into SHD's characteristics at the grid side of individual high-power DC EVSEs. This knowledge can contribute to the division of standards for the SH frequency range. Variations in time, operating condition, and resolution bandwidth, i.e. bin size are analyzed. Variations in operating conditions are also compared between multiple EVSEs. The EVSEs are tested against proposed limits to assess if they are realistic for high-power EVSEs. While not the focus, interesting phenomena outside of the SH range will also be mentioned.

In Section II, relevant concepts for supraharmonic analysis are explained. It also describes the conducted measurements and their motivation. Section III provides an overview of the measurement setup and lists the DUTs specifications. Section IV shows the collected spectra, spectrograms, and distortion per operating condition graphs. The graphs and their implications are described, as well. In Section V, conclusions from the measurement data are stated. Section VI lists the author's recommendations for future work.

II. Analysis

This section lists and explains what measurements are conducted and why certain choices are made. It also expands on SHC, TSHC, and the influence of grid impedance on current distortion.

A. SHC and TSHC

The SHC is analogous to the RBW of EMI receivers. Because of the analogy, some conclusions regarding the SHC can also be applied to the RBW. The SHC is described in Equation 1. It is the root sum square of all frequency components in the bandwidth between f_{min} and f_{max}. Choosing these values close to each other creates a bin with relatively low noise. However, if a bin is too small, a distortion with time-varying frequency could sometimes end up outside the bin. This leads to inconsistent results. Increasing the bin size increases the noise contribution, but decreases the likelihood of a distortion peak leaving the band. Another downside of a larger bin is that it increases the probability of multiple distortion peaks being in the bin. This is undesirable for the analysis of individual distortion peaks.

$$I_{SH} = \sqrt{\sum_{f=f_{min}}^{f_{max}} I_f^2} \tag{1}$$

Calculating the SHC with $f_{min} = 2$ kHz and $f_{max} = 150$ kHz results in the total supraharmonic current (TSHC). This quantity shows the total current in the SH spectrum. All frequencies contribute equally to the final value. Higher frequencies often have lower emission limits in standardization such as, for example, the Slangen limits. The reason is that higher frequencies tend to have more impact at equal magnitude than lower frequencies. Hence, the TSHC poorly summarizes an EVSE's impact because higher frequency distortions are under-represented.

B. Grid impedance

Grid impedance plays a vital role when measuring distortion. This is illustrated using Figure 1. It shows a simplified model of a 1-phase grid with an appliance modeled as a current distortion source and an impedance. The measured current distortion, i.e. the high-frequency current through Z_{grid}, decreases if the grid impedance increases. However, this does not mean a higher grid impedance is better, because it causes an increase in voltage distortion.

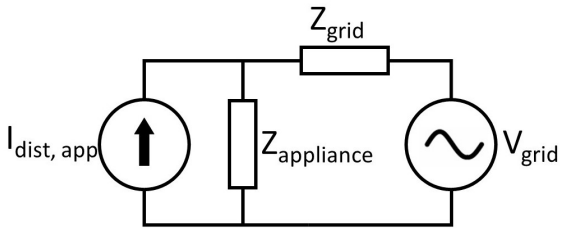

Fig. 1: Simplified model of a 1-phase grid with an appliance connected.

Because the grid impedance affects the measured current, comparing absolute values of SHC is only possible if the same grid impedance is used for each measurement. Usually, this is achieved by using a line impedance stabilization network (LISN). This device measures the current indirectly by measuring voltage over a predefined impedance. However, a LISN uses a lowpass filter to separate the distortion from the power-carrying frequency. Hence, a LISN works best at high-frequency distortion (150+ kHz). A different option is to measure current directly using current transducers. These devices work better at lower frequencies, compared to the LISN. Hence, they are more suitable for this research.

C. Frequency spectra

Frequency spectra of all EVSEs are used to compare the distortion characteristics of the EVSEs. The spectra are calculated by applying a 200 ms rectangular window to the center of a 500 ms measurement, after which the Fourier transform is calculated. The rectangular window does not attenuate the signal, but it does not prevent spectral leakage from occurring either. A 200 ms window results in a frequency resolution of 5 Hz after the Fourier transform is calculated, assuming a 1 MHz sampling frequency. The grid frequency must be divisible by the frequency resolution because distortion is expected at multiples of the grid frequency. A random frequency resolution would split these distortions over two frequency components, attenuating the magnitudes. The spectra's characteristics are anticipated to vary between EVSEs because they have different manufacturers that likely used different converters and EMI filters. The spectra are compared to the Slangen limits. A lower grid impedance allows higher limits, but no relation between the limit and the grid impedance is provided. Hence, 25% of the worst-case scenario of the installation limit is used as the individual device limit.

D. SHC characteristics at various operating conditions

The SHCs of 3 EVSEs are calculated for various DC currents and voltages to compare to the results found in [7]. The results are expected to be different since the EVSEs have different manufacturers and thus different converters and EMI filters. The measurements are performed as follows. Based on the specifications of the EVSE, a table with possible operating conditions is generated. Each operating condition is a unique combination of DC voltage and current. An example of the operating condition table is shown in Table I. Note that not all combinations of voltage and current are possible due to the EVSE's power limit.

TABLE I: Example of each operating condition's power for a 250 A, 1000 V, 180 kW EVSE. Conditions in red exceed this EVSE's power limit and can not be created.

DC Power (kW)		DC Current (A)				
		0	50	...	200	250
DC Voltage (V)	250	0	12.5	...	50	62.5
	300	0	15	...	60	75
	...	...	...	...	...	...
	700	0	35	...	140	175
	750	0	37.5	...	150	187.5
	800	0	40	...	160	200
	850	0	42.5	...	170	212.5
	900	0	45	...	180	225
	950	0	47.5	...	190	237.5
	1000	0	50	...	200	250

A 500 ms measurement is performed at each operating condition. The Fourier transform is calculated in the same way as stated above. Then, a bin around a dominant frequency component is selected to calculate the SHC. Since distortions could vary in frequency over time, the bin size is selected manually to ensure the peak remains in the bin. The bin sizes for EVSE 2 and 3 are determined recursively. The starting size depends on the presence of nearby distortions. For example, if the frequency to be analyzed is at 3 kHz, and distortion occurs at 2.95, 3, and 3.05 kHz, the starting bin size will be 50 Hz. If there is more space, the starting bin size is 200 Hz. The size is increased if the data shows that all measurements after a certain time show a significantly lower SHC, which is likely caused by the distortion leaving the bin. A sufficient bin size is reached if the significant drop in SHC is no longer present. If the significant drop does not vary over time when increasing the bin size, it is likely due to the charger's behavior, and a coincidence that the last measurements have significantly lower SHC. For example, an EVSE has 4 operating conditions that are measured consecutively. If the SHCs for the operating conditions are 35, 40, 5, and 3 for a 200 Hz bin, and 36, 41, 31, and 33 for a 500 Hz bin, the distortion probably left the 200 Hz bin between the second and third measurements.

E. Spectrogram

A 1-hour test where EVSE 1 supplies 650 V and 150 A is conducted to produce a spectrogram to examine slow spectral time variation. These variations can lead to time-dependent compatibility results. For example, the EVSE may pass the test in the first 5 minutes, but exceed the limits afterward. The test starts in the morning when the EVSE has not heated up from other tests. This is done so that potential temperature-related variation can be observed. During the test, a 500 ms measurement is performed every 20 seconds, resulting in 180 measurements. The spectra of all measurements are calculated identically to the way stated above. The spectrogram is produced by plotting all spectra in a 3D graph in chronological order.

III. Measurement Setup

This section describes the measurement setup, what equipment is used, and the specifications of the DUTs.

The measurement setup is illustrated in Figure 2. A script controls the charging discovery system (CDS) and the test computer. The CDS emulates a car starting a charging session and requests the EVSE for a certain voltage and current. The DC output current of the EVSE is not used to charge a car or battery, since these may contain uncontrollable variables like maximum charging current or the battery's state of charge. Instead, the power is fed to a DC emulator which converts the DC power to 3-phase AC power and feeds it back to the electricity grid. The AC grid emulators create a low-distortion 3-phase grid that powers the EVSE. A set of 5 Danisense DN1000ID current transducers is used to measure the currents in L1, L2, L3, N, and the PE cables. The transduced currents are sampled using a 24-bit 1 MS/s sample rate analog-to-digital converter with built-in shunts, which is part of the test computer. Unfortunately, only a test computer with a 16-bit 1 MS/s sample rate analog-to-digital converter was available for the measurements of EVSE 2. Hence, the noise floor in its spectra may be raised. The

specifications of all EVSEs can be found in Table II. The grid impedance of each phase to neutral at the EVSE's connection point is shown in Figure 17 in Appendix A.

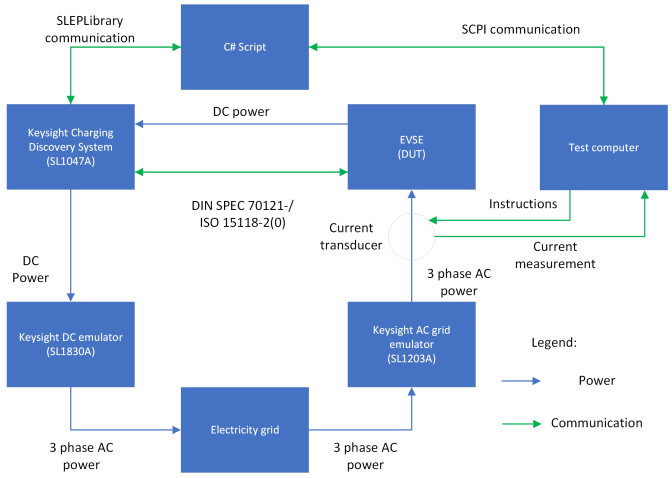

Fig. 2: Schematic overview of the measurement setup.

TABLE II: Specifications of the measured EVSEs.

	Voltage (V)	Max. Current (A)	Max. Power (kW)
EVSE 1	150 - 920	500	350*
EVSE 2	250 - 1000	250	180
EVSE 3	350 - 1000	500	150

**Limited by grid emulators. The practical limit is 330 kW.*

IV. Results

This section presents and discusses the collected measurement data. Each EVSE is discussed in a separate subsection. The results of the EVSEs are compared.

A. EVSE 1

Figure 3a and Figure 3b show EVSE 1's spectra while charging at 650 V, 0 A and 650 V, 500 A, respectively. The 500 A measurement has significantly higher distortion, which is unexpected as it contradicts findings in previous work. The spectrum in Figure 3b between 20 kHz and 40 kHz creates a hump-like shape, while Figure 3a shows little distortion in this range, aside from some narrowband peaks. Both figures show wideband distortion of similar magnitude around 90, 150, 212, 280, 338, 400, and 463 kHz. Figure 3a also shows wideband distortion around 30 kHz. This implies the fundamental distortion is at 30 kHz and only the odd harmonics of this 30 kHz distortion exceed the noise floor, which would result in steps of 60 kHz. The hump-like shape overshadows the 30 kHz distortion in Figure 3b, so it is not visible. Both figures also show a narrowband peak at exactly 240 kHz. Aside from the 150 kHz wideband distortion which exceeds the installation limit, the 0 A spectrum remains below 25% of the Slangen limit. The 500 A spectrum slightly exceeds the 25% limit at 10 kHz and 20 kHz and, like the 0A spectrum, it exceeds the installation limit at 150 kHz.

Fig. 3: EVSE 1: Frequency spectra.

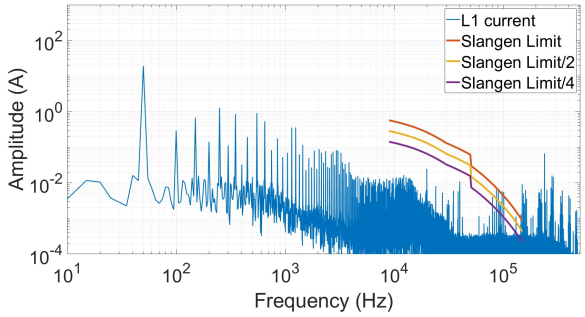

(a) EVSE 1: Frequency spectrum while supplying 650 V, 0 A.

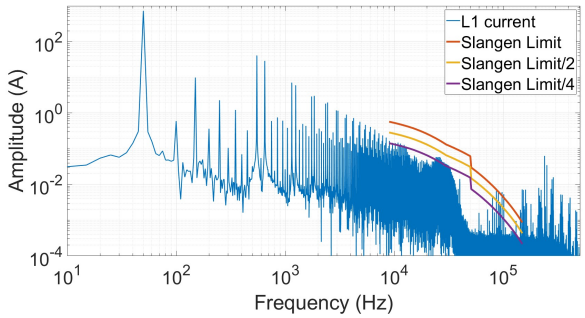

(b) EVSE 1: Frequency spectrum while supplying 650 V, 500 A.

Figure 4 shows the SHC of EVSE 1 in the 2.95 kHz bin with a bin size of 50 Hz. Constant power curves are included in the figure. The SHC increases both with an increase in DC current and DC Voltage. The SHC decreases at all measurement points around 250 kW. The constant power curves above 100 kW align with the SHC plot, which suggests the distortion is constant for constant power above 100 kW.

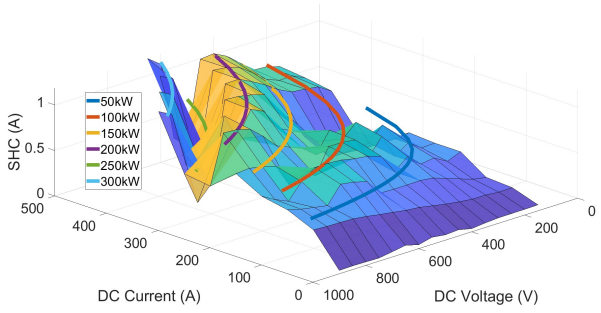

Fig. 4: EVSE 1: SHC in the 2.95 kHz bin and constant power lines.

Figure 5 shows Figure 4's datapoints sorted by power. Three trend lines are identified in red. The top two merge at 140

kW, and the bottom line merges with the others at 290 kW. Aside from the decrease in distortion between 250 and 300 kW, the SHC increases with power. The lines suggest the device's distortion fluctuates between three modes and is not completely random. The data does not show a clear relation between power and SHC in this frequency bin.

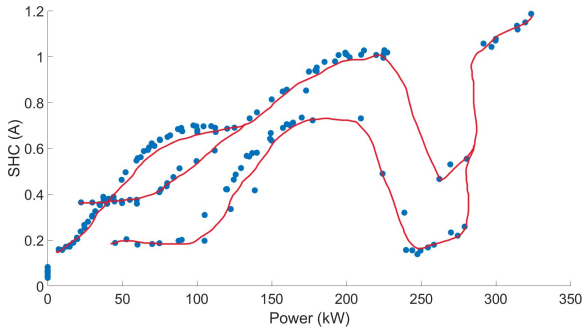

Fig. 5: EVSE 1: SHC in the 2.95 kHz bin against power in blue and trend lines in red.

Figure 6 shows the 24.5 - 26.5 kHz range of the spectrogram which resulted from the 1-hour 650 V, 150 A measurement of EVSE 1. It contains an odd harmonic of the 50 Hz grid frequency every 100 Hz. These are present in the spectrogram between 0 and 48 kHz with decreasing amplitude over frequency. Figure 6 also contains a "traveling" distortion that decreases 2 kHz in frequency during the measurement. The frequency change rate decreases over time. Determining if the amplitude of the traveling distortion is constant is difficult as it crosses the frequency-stable harmonic distortion peaks. The harmonics can cause constructive or destructive interference with the traveling signal, depending on their relative phase.

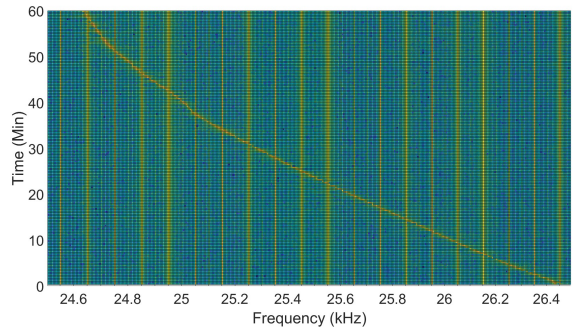

Fig. 6: EVSE 1: Spectrogram from 24.5 to 26.5 kHz while charging at 650 V, 150 A.

Figure 7 shows the 71.0 - 73.0 kHz range. It shows a magnitude-varying distortion peak at exactly 72 kHz. The changes are not repetitive, but rather random.

Figure 8 shows the 87.3 - 89.2 kHz range. It shows a single traveling distortion peak that changes its frequency by 1.7 kHz

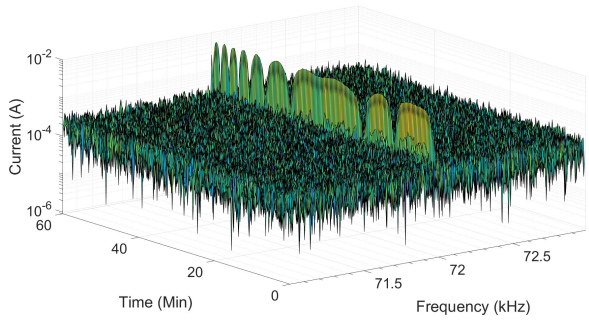

Fig. 7: EVSE 1: Spectrogram from 71.0 to 73.0 kHz while charging at 650V, 150A.

over the 1-hour measurement. The frequency change seems gradual, but a small bump occurs at 40 minutes. This bump is also visible in Figure 6. Although the 88 kHz and 25 kHz traveling peaks have a similar shape, they cannot be some harmonic of the same fundamental. If they were, the frequency change over time of the 88 kHz traveling peak should be 88/25 higher than the frequency change of the 25 kHz peak, which it is not.

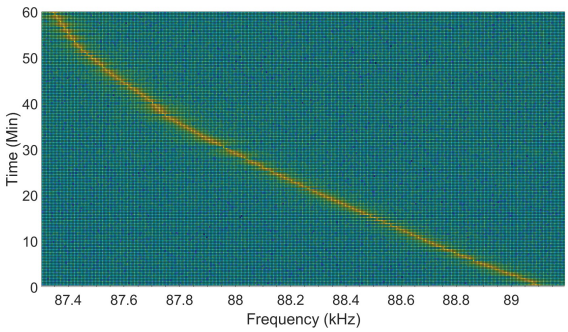

Fig. 8: EVSE 1: Spectrogram from 83.3 to 89.2 kHz while charging at 650 V, 150 A.

Figure 9 shows the 98.8 - 100.8 kHz range. It contains a traveling peak that increases by 1.9 kHz over the 1-hour measurement. Its shape is again similar to the 88 kHz and 25 kHz traveling peak, including the bump at 40 minutes, but its frequency increases, instead of decreases.

Figure 10 shows EVSE 1's SHC over time for various bin sizes of the distortion shown in Figure 8. Selecting the larger binsize suggests the peak's amplitude is stable, which is correct. Selecting a smaller bin size suggests the magnitude is time-dependent, which is incorrect. Notice that when the distortion is inside the small bin, the larger bin remains higher because of the extra noise components. In compliance testing, static bands are measured consecutively. This means that if the frequency sweep speed of the EMI receiver matches the speed at which the distortion changes frequency, a narrowband distortion like in Figure 9 is observed as a 2 kHz distortion band by the

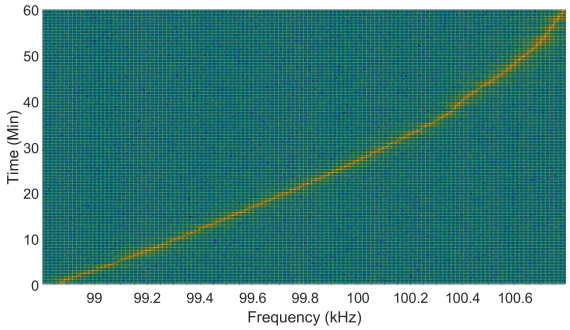

Fig. 9: EVSE 1: Spectrogram from 98.8 to 100.8 kHz while charging at 650V, 150A.

EMI receiver. This is one of many issues that can occur with frequency-varying distortion and consecutive compliance testing. The distortion's frequency can also increase slower than the frequency sweep speed. Or the distortion frequency could decrease. All these scenarios lead to different problems that cause time-dependent compatibility results. Although Figure 10 suggests a sufficiently large RBW solves these problems, this is only true if the band's center frequency is chosen such that all frequencies at which the distortion can occur are inside the band. This is hard to achieve without manually inspecting the data. Hence, it is hard to implement in standardized compliance tests. A solution is to have an overlap between bands. This way, the frequency-varying distortion will always be detected. However, this can still make the distortion appear more wideband than in reality. Besides, introducing overlap increases the compliance test duration, which is undesirable. A different solution is to measure all frequencies simultaneously using, for example, a time-domain EMI receiver. This way, only the observed distortion's frequency can vary, but the amplitude is constant.

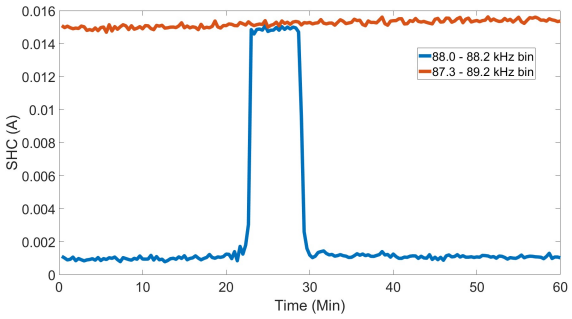

Fig. 10: EVSE 1: L1's SHC over time for varying bin sizes while constantly charging 650 V, 150 A

Figure 11 shows the TSHC of the 1-hour measurement. The TSHC increases by 3% during the test, with the most significant change happening in the first 10 minutes. After 1 hour, the maximum TSHC difference between phases is 1.7%. Although these changes are small, they can make the difference between passing or failing a compliance test. Hence, more research is required to determine what causes the deviation. Does it only occur if the EVSE is turned on right before the test, or does it also happen if the EVSE has been in standby mode for some time? Do all EVSEs exhibit this behavior? Since the data shows a difference between phases, it is recommended to do compliance testing on all phases.

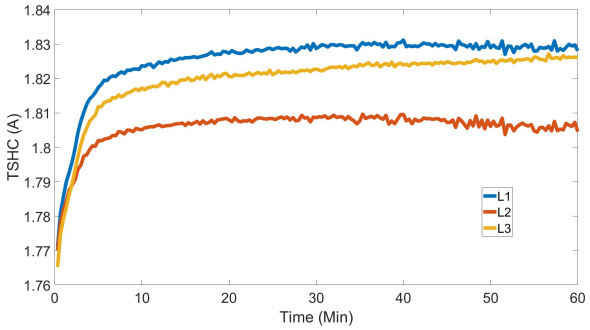

Fig. 11: EVSE 1: TSHC over time.

B. EVSE 2

Figure 12 shows the spectrum of EVSE 2 while charging at 950 V, 150 A. Notice that the noise floor is raised because of the 16-bit analog-to-digital converter. It exceeds the Slangen limits at higher frequencies. The spectrum shows harmonics up to roughly 5 kHz. It also shows narrowband distortion at 22 and 44 kHz. Since the 22 kHz distortion is the highest (aside from harmonic distortion), it is most likely the converter's switching frequency. The 44 kHz distortion is probably the switching frequency's second harmonic. A large distortion is present at 240 kHz. The spectrum also shows wideband distortion at several frequencies starting at 100 kHz. However, they are difficult to analyze because of the raised noise floor. The distortion at 22 kHz, 44 kHz, and 100 kHz exceed the installation level Slangen limit.

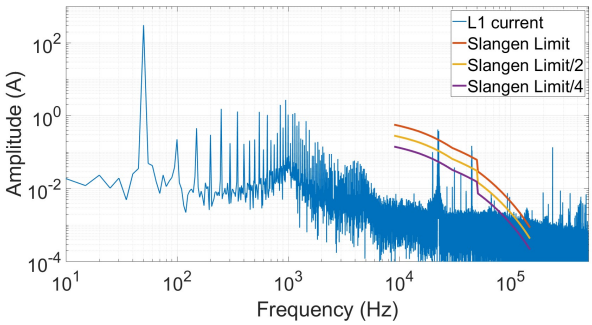

Fig. 12: EVSE 2: Frequency spectrum while charging at 950 V, 150 A.

Figure 13 shows EVSE 2's SHC per operating condition in the 22 kHz bin. The data shows a weak correlation between DC current and SHC.

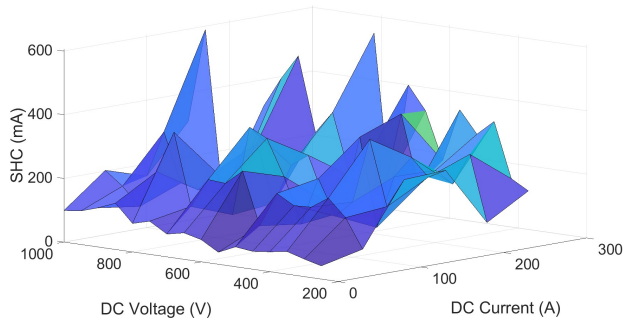

Fig. 13: EVSE 2: SHC in the 22.335 kHz bin.

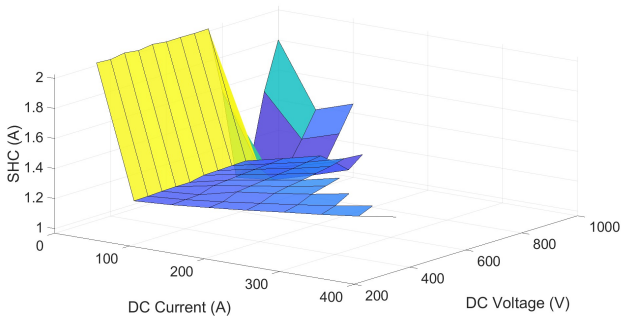

Fig. 15: EVSE 3: SHC in the 18 kHz bin.

C. *EVSE 3*

Figure 14 shows the spectrum of EVSE 3 while charging at 450 V, 0 A. Two distortion shapes are identified. The first is the largest peak at 18 kHz and all its harmonics up to 108 kHz. These distortion ranges have a high middle and decrease with distance from the center of the distortion. The second distortion shape, which has a flat top, is found at 150.3 kHz and every interval of precisely 62.7 kHz afterward. It is possible that this shape would be at 87.6 kHz, but it overlaps with the 5th harmonic of the switching frequency at 90 kHz, so this is unclear. At 87.6 - 62.7 = 24.9 kHz, another peak is present. This is likely a coincidence. The difference of all peaks is 62.7 kHz, so the fundamental must be either 62.7 or 31.35 kHz. No distortion shows at 62.7 kHz, but there is a narrow peak at 31.35 kHz. However, this peak does not have the same shape as the wideband distortion at the higher frequencies.

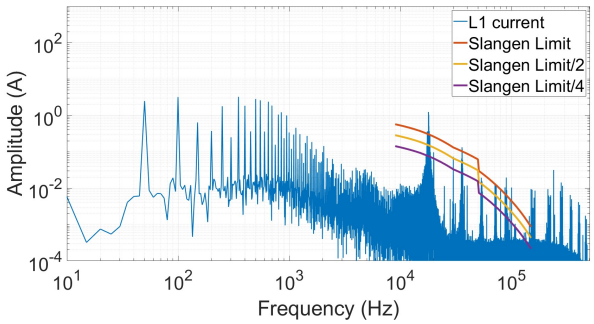

Fig. 14: EVSE 3: Frequency spectrum while charging at 450 V, 0 A.

Figure 15 shows the SHC in the 18 kHz bin with a bin size of 2 kHz of EVSE 3 relative to the current and voltage. The distortion is highest while charging with 0 A below 800 V. From 50 A, the SHC increases with current. The distortion is lowest between 850 and 900 V.

Figure 16 increases the DC current resolution in the 0 - 50 A range. The SHC is raised significantly if the EVSE is charging at 0 A. If a charging plaza with only this type of EVSE must temporarily interrupt charging due to grid congestion, the SHD emitted to the grid could become substantial.

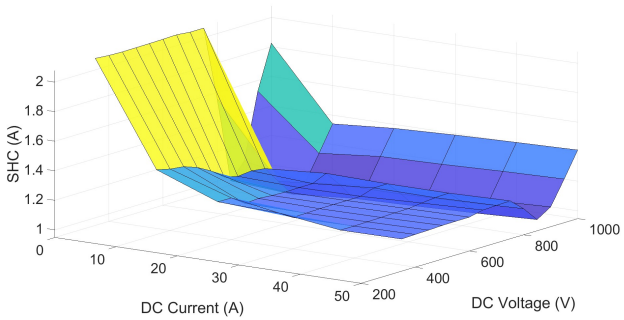

Fig. 16: EVSE 3: SHC in the 18 kHz with higher DC current resolution.

D. *Comparisson*

The spectra of EVSE 2 and 3 are similar, which was unexpected. They both contain a single dominant, narrowband frequency component and its harmonics. EVSE 1's spectrum differs from the others as anticipated, since it mainly contains wideband distortion.

The wideband high-frequency distortions are present in EVSE 1 and 3 and occur at similar frequencies. It seems they are also present in EVSE 2's spectrum, although it is hard to see due to the raised noise floor. It is assumed they are caused by the measurement setup because they occur in all presented spectra at similar magnitudes, while other parts of the spectra vary from each other. The same goes for the 240 kHz distortion. Since the 100 kHz distortion is assumed to be caused by the measurement setup, EVSE 1 complies with the installation level Slangen limit, and nearly with the 25% limit. EVSE being the closest to compliance is unexpected as it is the highest power EVSE. Since EVSE 1 nearly complies with the 25% limit, they seem realistically achievable for EVSE manufacturers.

The characteristics of the EVSEs' SHC per operating condition vary significantly, as expected. EVSE 1's SHC seems to increase with power, EVSE 2's SHC appears to lack any correlation, and EVSE 3's SHC seems highest when supplying 0 A.

V. Conclusion

Three EVSEs have been measured to characterize their SHD at the grid side. The knowledge can contribute to the division of standards for the SH frequency range. Aside from 2 EVSEs showing similar spectra, the data showed significant differences between EVSEs in spectral behavior and SHC characteristics for various operating conditions. The measurements also indicated that distortion can vary in frequency and amplitude over time. The EVSEs have also been tested against the Slangen limits assuming the grid emulators had a relatively high impedance. Two EVSEs exceeded the installation limit. However, the EVSE with the highest power almost remained within the individual device limit. Hence, the individual device limit seems feasible.

VI. Recommendations

This section lists the author's future work recommendations.

- It is recommended to research under what conditions the time-dependent emissions of EVSEs occur, and if these can be removed from a standardized compliance test.
- More research is required on how the RBW influences the repeatability of compliance test results in the SH range, and if band overlap or time domain EMI receivers are (feasible) solutions.

References

[1] T. M. H. Slangen et al. "The Harmonic and Supraharmonic Emission of Battery Electric Vehicles in The Netherlands". In: *2020 International Conference on Smart Energy Systems and Technologies (SEST)*. 2020, pp. 1–6. DOI: 10.1109/SEST48500.2020.9203533.

[2] Frank Leferink. "Conducted Interference, Challenges and Interference Cases". In: *IEEE Electromagnetic Compatibility Magazine* 4.1 (2015), pp. 78–85. DOI: 10.1109/MEMC.2015.7098517.

[3] *CENELEC SDC 205A Study Report on Electromagnetic Interference between Electrical Equipment/Systems in the Frequency Range below 150 kHz*. Tech. rep. SC205A/Sec0329/DC. CENELEC, March 2013.

[4] Sarah K. Rönnberg et al. "On waveform distortion in the frequency range of 2kHz–150kHz—Review and research challenges". In: *Electric Power Systems Research* 150 (2017), pp. 1–10. ISSN: 0378-7796. DOI: https://doi.org/10.1016/j.epsr.2017.04.032. URL: https://www.sciencedirect.com/science/article/pii/S0378779617301864.

[5] IEC-61000-4-7:2002/A1:2009. *Electromagnetic compatibility (EMC) - Part 4-7: Testing and measurement techniques - General guide on harmonics and interharmonics measurements and instrumentation for power supply systems and equipment connected thereto*. 2009.

[6] T. M. H. Slangen et al. *Standards for 2-150 kHz*. Tech. rep. TEPQEV, 2023. URL: https://elaad.nl/wp-content/uploads/downloads/TEPQEV-Whitepaper-standardization-20230228.pdf.

[7] Tim Slangen et al. "Variations in Supraharmonic Emission (2-150 kHz) of an EV Fast Charging Station under Different Supply- and Operating Conditions". English. In: *2023 IEEE Power & Energy Society General Meeting (PESGM)*. 2023 IEEE Power & Energy Society General Meeting (GM) ; Conference date: 16-07-2023 Through 20-07-2023. United States: Institute of Electrical and Electronics Engineers, Sept. 2023, pp. 1–5. DOI: 10.1109/PESGM52003.2023.10252962.

[8] Jon González-Ramos et al. "Emissions generated by electric vehicles in the 9-500 kHz band: Characterization, propagation, and interaction". In: *Electric Power Systems Research* 231 (2024), p. 110289. ISSN: 0378-7796. DOI: https://doi.org/10.1016/j.epsr.2024.110289. URL: https://www.sciencedirect.com/science/article/pii/S0378779624001779.

APPENDIX A
GRID IMPEDANCE MEASUREMENT

Figure 17 shows the measured grid impedance at the EVSE's point of connection, which means the impedance of the cables is included. It shows an inductive impedance. 4 AC grid emulator (ACE) modules were used for the EVSE 1 measurements, as 3 ACE modules could not provide enough power. During the measurements of EVSE 2 and 3, only 3 ACE modules were used.

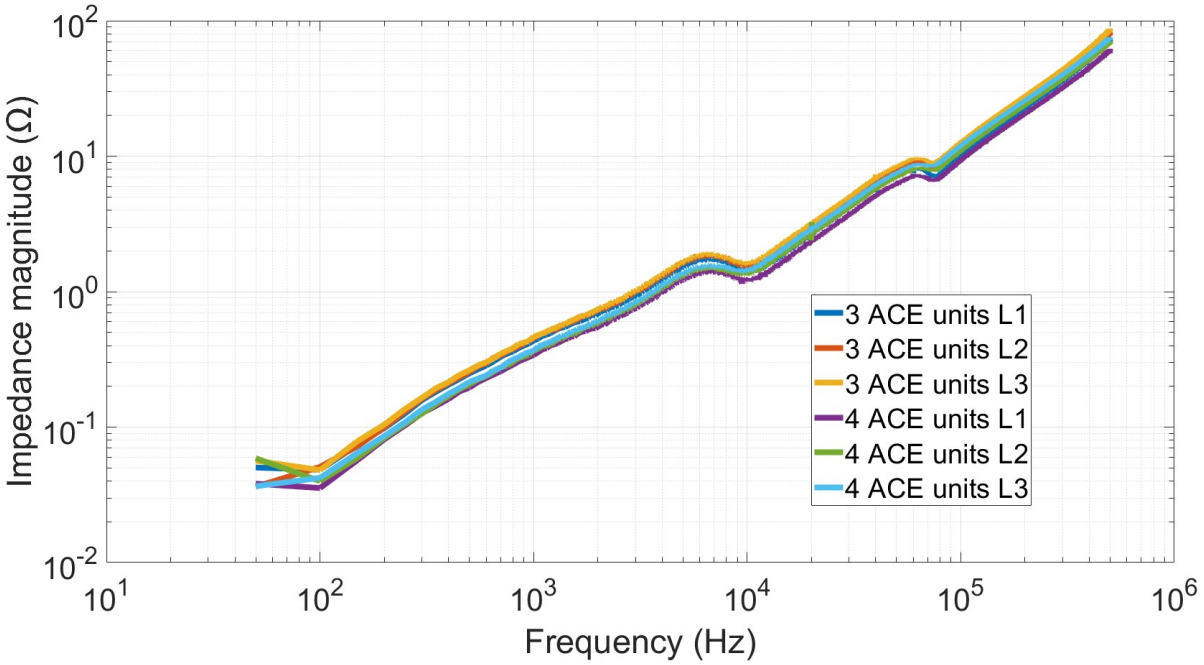

Fig. 17: Measured impedance of the grid emulator with no load connected.